NeuroImage: Clinical 20 (2018) 594–602

Contents lists available at ScienceDirect

NeuroImage: Clinical

journal homepage: www.elsevier.com/locate/ynicl

Callosal and subcortical white matter alterations in schizophrenia: A diffusion tensor imaging study at multiple levels

Wei Zhao[a], Shuixia Guo[a,b,*], Ningning He[a], Albert C. Yang[d,e,f,g], Ching-Po Lin[c,g,h], Shih-Jen Tsai[d,e,g,**]

[a] College of Mathematics and Statistics, Key Laboratory of High Performance Computing and Stochastic Information Processing (Ministry of Education of China), Hunan Normal University, Changsha, PR China
[b] Key Laboratory of Molecular Epidemiology of Hunan Province, School of Medicine, Hunan Normal University, Changsha, PR China
[c] Aging and Health Research Center, National Yang-Ming University, Taipei, Taiwan
[d] Department of Psychiatry, Taipei Veterans General Hospital, Taipei, Taiwan
[e] Division of Psychiatry, School of Medicine, National Yang-Ming University, Taipei, Taiwan
[f] Division of Interdisciplinary Medicine and Biotechnology, Beth Israel Deaconess Medical Center/Harvard Medical School, Boston, USA
[g] Institute of Brain Science, National Yang-Ming University, Taipei, Taiwan
[h] Institute of Neuroscience, National Yang-Ming University, Taipei, Taiwan

ARTICLE INFO

Keywords:
Schizophrenia
Diffusion tensor imaging
White matter
Fractional anisotropy
Structural network

ABSTRACT

Diffusion tensor imaging and its distinct capability to detect micro-structural changes *in vivo* allows the exploration of white matter (WM) abnormalities in patients who have been diagnosed with schizophrenia; however, the results regarding the anatomical positions and degree of abnormalities are inconsistent. In order to obtain more robust and stable findings, we conducted a multi-level analysis to investigate WM disruption in a relatively large sample size (142 schizophrenia patients and 163 healthy subjects). Specifically, we evaluated the univariate fractional anisotropy (FA) in voxel level; the bivariate pairwise structural connectivity between regions using deterministic tractography as the network node defined by the Human Brainnetome Atlas; and the multivariate network topological properties, including the network hub, efficiency, small-worldness, and strength. Our data demonstrated callosal and subcortical WM alterations in patients with schizophrenia. These disruptions were evident in both voxel and connectivity levels and further supported by associations between FA values and illness duration. Based on the findings regarding topological properties, the structural network showed weaker global integration in patients with schizophrenia than in healthy subjects, while brain network hubs showed decreased functionality. We replicated these findings using an automated anatomical labeling atlas to define the network node. Our study indicates that callosal and subcortical WM disruptions are biomarkers for chronic schizophrenia.

1. Introduction

Schizophrenia, as a complex disease, is characterized by different symptoms, including a combination of emotional and cognitive disturbances in various functions, such as in emotional experience and expression, inferential thinking, language, and perception (Andreasen et al., 1994). As normal brain functions are served by macro-structural circuits of cortical and subcortical areas, the core pathology of schizophrenia is possibly caused by the dysconnectivity within and between brain regions (Peters et al., 2010). Brain white matter (WM) is key to neural communication, as it contains axonal projections to other neurons and functional brain areas; therefore, dysconnectivity in schizophrenia could result from WM lesions (Domen et al., 2013; Karlsgodt, 2015).

As a modified technique of magnetic resonance imaging (MRI), diffusion tensor imaging (DTI) is used to characterize the main WM fiber bundles *in vivo* (Guo et al., 2012a; Kong et al., 2011; Zhao et al., 2017). The exploration of WM disruptions using DTI is featured at different levels, ranging from the degree of water diffusion anisotropy of single voxels (uni-variate), to the anatomical connectivity between

* Correspondence to: S. Guo, College of Mathematics and Statistics, Key Laboratory of High Performance Computing and Stochastic Information Processing (Ministry of Education of China), Hunan Normal University, Changsha, PR China.
** Correspondence to: S. J. Tsai, Department of Psychiatry, Taipei Veterans General Hospital, Taipei, Taiwan.
E-mail addresses: guoshuixia75@163.com (S. Guo), tsai610913@gmail.com (S.-J. Tsai).

https://doi.org/10.1016/j.nicl.2018.08.027
Received 6 May 2018; Received in revised form 25 July 2018; Accepted 20 August 2018
Available online 24 August 2018

pairwise brain regions (bi-variate), and then to the coordinated pattern of connectivity between several brain regions (multi-variate) (Peters et al., 2010). A unique dimension is accessible for each level to explore WM disruption in patients. At the lowest level, the degree of water diffusion anisotropy concerning a single voxel is broadly applied for assessing the integrity of the underlying brain tissue (Samartzis et al., 2014), and these diffusion parameters include fractional anisotropy (FA), mean diffusivity (MD), radial diffusivity (RD) and axial diffusivity (AD). FA is the most commonly used DTI measurement (Karlsgodt et al., 2015). Reduced FA is possibly related to fewer crossing or coherent fibers, thinner myelin sheaths, decreased axonal diameter, and decreased number of axons within a voxel (Kubicki et al., 2007; Samartzis et al., 2014). At this level, a large number of studies have reported positive findings (see review Fitzsimmons et al., 2013). For example, Guo et al. (2012b) found lower FA values in right-sided WM tracts of cortical and subcortical regions. Roalf et al. (2013) found decreased FA values in a large portion of the corpus callosum. At intermediate levels, pairwise WM anatomical connectivity can be reconstructed by adopting diffusion tractography methods (Bassett et al., 2008). Previous research has indicated that DTI deterministic tractography findings on WM tracts are consistent with known WM anatomy (Wakana et al., 2004).The direct investigation of axonal connectivity by examining all voxels jointly, instead of each voxel separately, as well as the present pathophysiological theories regarding schizophrenia highlight that the complicated clinical presentations of schizophrenia are not caused by abnormalities in a certain focal region but in inter-regional interactions (Bullmore et al., 1997; Stephan et al., 2006; Wang et al., 2012). At higher levels, based on a complicated network theory, the multivariate pattern of structural interactions is examined between brain areas. It seems that network organization in patients with schizophrenia, as extracted from various imaging modalities (DTI, fMRI, and sMRI), is random and less cost-efficient than in healthy individuals (Bassett et al., 2008, 2009, 2012; Wang et al., 2012).

Several researchers have investigated WM lesions in patients diagnosed with schizophrenia at the respective level. However, some results are inconsistent and even opposite among previous reports. For instance, by using fiber tracking approaches or voxel-based analysis (VBA), some researchers have demonstrated widespread WM abnormalities, while others have suggested there are no such differences between patients with schizophrenia and healthy individuals (for a review, see Fitzsimmons et al., 2013). The major reason for these opposite findings is the rather small experimental data sets. Based on recent reviews (Liu et al., 2017; O'Donoghue et al., 2017), only a few studies have collected more than a hundred samples from schizophrenia patients. Recently, a study (Kelly et al., 2017) collected 4322 individuals from 29 cohorts to investigate WM disruptions in schizophrenia; they found widespread significantly lower FA values in patients, especially in the anterior corona radiata and corpus callosum. This study was based on a large sample of VBA and revealed robust WM abnormalities. However, VBA allows comparisons for each voxel without connectional information, and because of the diffuse nature of localized findings, it can be difficult to determine the fibers which traverse these areas and are affected by a localized disruption in WM (Zalesky et al., 2011). Hence, for verifying the results simultaneously from a single voxel level and a connection level, we combined two important but previously separate approaches, VBA and diffusion tractography, to examine the uni-, bi-, and multi-variate properties and identify WM abnormalities in schizophrenia. The steps of the multilevel approach included: (1) the use of VBA applied to FA measurements and correlation of the findings with symptom severity; (2) construction of a structural network for each subject using a WM tracking algorithm to investigate the patients' connectivity impairments, as a way of confirming the FA results; and (3) comparison of the topological properties of the structural network in patients and healthy subjects. Each method provides knowledge on an aspect of the disease; thus, the combination of these diverse analytical clues is important to form a more comprehensive outlook of the pathology of schizophrenia.

Table 1
Subject demographics.

Characteristics	Patient	Control	p value
	(n = 142)	(n = 163)	
Male/female	59/83	71/92	0.72
Age(year)	43.8 ± 10.9	42.1 ± 11.1	0.16
Education(year)	12.5 ± 3.5	15.9 ± 3.5	< 0.001
Duration(year)	16.6 ± 10.1	/	/
PANSS positive scale score	9.5 ± 3.1	/	/
Negative scale score	9.7 ± 4.7	/	/
General psychopathology score	20.5 ± 4.3	/	/
Total score	39.7 ± 9.7	/	/

Note: PANSS positive and negative symptom scale.

2. Materials and methods

2.1. Subjects

One hundred and forty-two patients with chronic schizophrenia (59 males and 83 females) were recruited for this study and they were identified according to the DSM-IV diagnostic criteria by qualified psychiatrists at the Taipei Veterans General Hospital. Exclusion criteria included the presence of DSM-IV Axis I diagnoses of other disorders such as bipolar disorder, history of any substance dependence or history of clinically significant head trauma. Illness durations ranged from several months to 40 years (mean ± SD: 16.6 ± 10.1 years). All patients were being treated with a range of antipsychotics. Their average age was 43.8 ± 10.9 years and they had a mean education duration of 12.5 ± 3.5 years. Symptom severity was measured using the Positive and Negative Syndrome Scale (PANSS) assessment which was given to all schizophrenic participants either one week before the MRI scan or one week after it. All patients complete their PANSS assessment as listed in Table 1.

One hundred sixty three (71 male and 92 female) healthy control subjects were also recruited. Their average age was 42.1 ± 11.1 years, and their mean education duration was 15.9 ± 3.5 years. All of the controls were assessed in accordance with DSM-IV criteria as being free of schizophrenia and other Axis I disorders. None of them had any neurological diseases or suffered from clinically significant head trauma and none had a history of any substance dependence. The patient and control groups were well matched by gender (chi-square test, $p = 0.72$) and age (two samples t-test, $p = 0.16$) although the controls had a slightly longer education duration (two samples *t*-test, $p < 0.001$). Patient and healthy control demographics are shown in Table 1.

All the patients were diagnosed according to the Diagnostic and Statistical Manual of Mental Disorders-IV criteria, then administered a diagnostic structured Mini- International Neuropsychiatric Interview (MINI), Mini-Mental State Examination (MMSE) Chinese version. The cognitive functioning of the participants was evaluated using the MMSE for general cognitive status and the Wechsler Digit Span subtest for verbal working memory abilities. All participants exhibited sufficient visual and auditory acuity to undergo cognitive testing. This study was conducted in accordance with the Declaration of Helsinki and approved by the Institutional Review Board of Taipei Veterans General Hospital. Written informed consent was obtained from all participants ensuring adequate understanding of the study. Any participants with the presence of possible dementia or illiteracy were excluded.

DTI data and T1-weighted 3D high-resolution brain images were acquired for each subject on a 3 T MR system (Siemens Magnetom Tim Trio, Erlangen, German) at National Yang-Ming University, equipped with a high-resolution 12-channel head array coil (see Supplement for acquisition parameters).

2.2. Data analysis

2.2.1. Preprocessing

The PANDA toolbox was adopted to preprocess DTI data (Cui et al., 2013). In the original DTI data, an affine alignment was applied for the registration of other diffusion images to b0 images, which could correct the influence of head motion and image distortion resulting from eddy currents. A linear least-squares fitting method was applied for estimating the diffusion tensor metrics. FA maps were first created for each subject. There are several studies (Baum et al., 2018; Yendiki et al., 2014) that have suggested the importance of motion correction in DTI measures. In this study, we used four head motion parameters including average volume-by-volume translation, average volume-by-volume rotation, percentage of slices with signal drop-out, and signal drop-out severity, using the TRAUCULA algorithm (Yendiki et al., 2011) implemented in FreeSurfer (See supplementary materials for details, and Fig. S1 for these four DTI head motion parameters for all subjects). Because the two groups were significantly different in the head motion measures (Table S3), we included these measures as a nuisance regressor in the group comparison.

2.2.2. Univariate voxel based analysis

To assess differences in FA maps between schizophrenia patients and controls on the voxel-by-voxel basis, VBA was performed (Deprez et al., 2012). According to the standard FMRIB58_FA 1 mm template, FA maps were standardized for every subject and an average FA map was produced according to the Montreal Neurological Institute (MNI) atlas space. Then, the average FA map was limited to an FA value of 0.2 so that the analysis could be confined to the WM, and a 6-mm full width at half maximum Gaussian kernel was used to smooth the standardized FA maps for comparisons among groups. In WM mask, voxel-wise permutation based nonparametric inference (Winkler et al., 2016) was performed on FA data adjusted for head motion parameters and age, using Data Processing and Analysis of Brain Imaging toolbox (Yan et al., 2016) with 5000 permutations.

For clusters that showed significant between-group differences in FA values, we calculated Spearman's correlation between the mean FA value in each significant cluster and the clinical measures for each patient, including the duration of illness, the total score on the Positive and Negative Syndrome Scale (PANSS; total score, PANSS_t) and the scores on the PANSS positive subscale (PANSS_p), the PANSS negative subscale (PANSS_n), and the PANSS general subscale (PANSS_g).

2.2.3. Network construction

2.2.3.1. Definition of network node. The anatomical network of human brain was established according to the Human Brainnetome (BN) Atlas (Fan et al., 2016), which parcellates the brain into 246 regions of interest (ROIs). Supplementary Table 1 lists the names and abbreviations for these regions. Every ROI was defined as a node with a structural connection which can be identified between every pair of nodes as an edge. With the usage of an affine transformation, the T1-weighted structural images were co-registered to their according FA native diffusion spaces. Then, with the application of non-linear transformation (FSL/FNIRT tool), the individual transformed structural images were standardized in accordance with the ICBM-152 template. Based on the method of nearest-neighbor interpolation, the template in the MNI space was warped to the native diffusion space through an inverse transformation (Gong et al., 2009; Wen et al., 2011).

2.2.3.2. Definition of network edge. We carried out whole-brain fiber tracking in native diffusion space for every subject, by using the Fiber Assignment by Continuous Tracking algorithm (FACT) (Mori et al., 1999). Streamlines were drawn from every voxel following the main diffusive direction for the reconstruction of WM fibers. In case that the angle between the eigenvectors of two consecutive voxels was larger than 45, or the FA was < 0.2, the tracking was stopped. The number of axonal fibers connecting two brain regions was used to define the edge weight. In this way, a 246×246 symmetric weighted connectivity matrix was obtained for each subject. Next, we identified a group-wise network, *i.e.*, a network in which connections were most consistent across subjects in each group, by using one-tailed sign test. After that, we applied the Bonferroni method to correct for multiple comparisons at $p < 0.05$. Therefore, the group-wise network was detected in patients and controls.

2.2.4. Bivariate connectivity analysis

The individual weighted matrix was constructed as described previously. Next, in order to identify impaired subnetworks in patients, we performed network-based statistic (NBS) analysis (Zalesky and Fornito Abullmore, 2010). The total number of streamlines that interconnected the nodes was used to quantify the connectivity between pairs of nodes. In performing the NBS calculations, the primary threshold for each inter-regional connection in connected subnetwork was set to a t value > 2.6 or $p < 0.005$ (5000 permutations). Contrasts for both controls > patients and patients > controls were tested.

2.2.5. Multivariate connectivity analysis

Single-subject connectivity matrices were binarized if the fiber number between a pair of ROIs was ≥ 1. In this way, a symmetric 246×246 binary matrix representing the brain anatomical network for each subject was obtained. Graph theory was used to analyze the topological characteristics of human brain anatomical networks. The global characteristics of the networks were measured using the following parameters: degree (K_p), network strength (S_p), global efficiency (E_{glob}), local efficiency (E_{loc}), and small-worldness (σ). The detailed description of these topological parameters is presented in Supplementary Materials and also in Bullmore and Bassett (2011). In addition, the hub regions for each group were detected based on the group-wise network, and a region was defined as a hub if its nodal degree appeared among the top 5% largest among the 246 regions. We performed the network analysis using the GRETNA software (Wang et al., 2015).

2.3. Robustness of the network analysis

The robustness of our main findings was estimated by employing another parcellation scheme, known as the automated anatomical labeling atlas (AAL) (Tzourio-Mazoyer et al., 2002), which contains 90 ROIs. Region names and abbreviations are listed in Supplementary Table 2. Then, the bivariate connectivity analysis and multivariate connectivity analysis were repeated as described above.

3. Results

3.1. Univariate voxel analysis: fractional anisotropy

The patients showed widespread significantly lower FA values than healthy subjects, with cluster size ≥ 40 and threshold at $p < 0.01$ (family-wise error rate corrected; Fig. 1). The number of voxels for each white matter tract is shown in Table 2. Regions included corpus callosum (genu, body, splenium), cerebral peduncle bilaterally, limb of internal capsule (anterior, left posterior), fornix, right external capsule and superior cerebellar peduncle bilaterally. Neither of these regions showed higher FA values in patients than in healthy subjects.

Spearman-rank correlation between mean FA values of significant clusters and the clinical measures of each patients was examined. The results are summarized in Table 3. We found statistically significant associations between the averaged FA values in the right external capsule (EC.R) and PANSS_n and PANSS_t in schizophrenics. As the psychiatric symptoms became more severe among patients, the values of FA became lower in this region. In addition, the duration of illness negatively correlated with mean FA values in the corpus callosum (genu

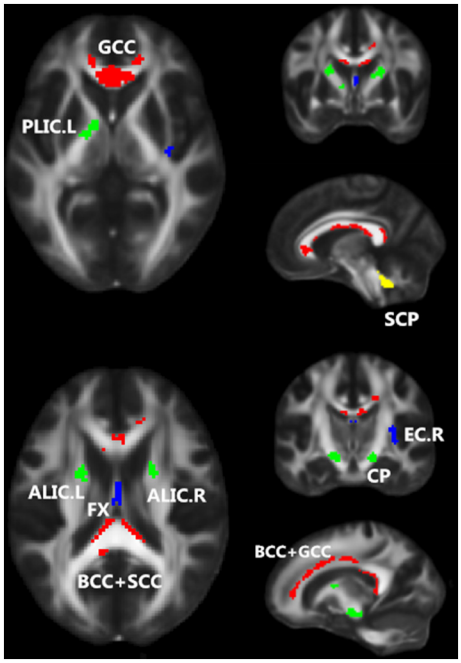

Fig. 1. Regions showing significantly lower FA values in patients with schizophrenia (n = 142) than in healthy subjects (n = 163). Regions that belong to the commissural fibers, projection fibers, association fibers, and tracts in the brainstem are color-coded in red, green, blue, and yellow, respectively. These results are adjusted for motion score and age. Note: L, left hemisphere; R, right hemisphere.(For interpretation of the references to color in this figure legend, the reader is referred to the web version of this article.)

and body) and left limb of the posterior internal capsule (PLIC.L), consistently with a previous meta-analysis of first-episode and multi-episode studies showing that more severe WM abnormalities are related to longer disease duration (Bora et al., 2011).

3.2. Bivariate connectivity analysis

Fig. 2(a) demonstrates the group-wise network for patients and healthy subjects. With the application of a one-tailed sign test (p = 0.05, Bonferroni correction), the inter-regional connections totaled 1733 for the patients and 1976 for the healthy subjects. Moreover, the sparsity of structural connectivity (SC) for healthy subjects (0.0656) was 12.3% larger than that for patients (0.0575).

Fig. 2(b) displays the two impaired subnetworks identified using the NBS method. [p = 0.05, family-wise error rate corrected]: one subnetwork consisted of 26 connections mainly including connections between and within frontal and subcortical areas (p = 0, corrected), and another consisted of 5 connections mainly including connections between and within parietal and subcortical regions (p = 0.0112, corrected). The details of all the 31 inter-regional connections are listed in Supplementary Table 4. We noticed dramatically lower values of all connections in patients than in healthy individuals. These connections involved three regionally distinct node groups: the frontal (especially the superior frontal gyrus), parietal (especially the superior parietal lobule and precuneus), and subcortical (especially the thalamus) nodes. In patients, multiple transcallosal pathways [Fig. 2(c); 10 connections among all 31 impaired connections] interconnecting with contralateral nodes within the frontal and parietal groups were disrupted. Interestingly, four homotopic connections were included; three in the frontal region and one in the parietal, consistently with our VBA results, which demonstrated a significant reduction in the FA value in the corpus callosum. Subcortical-cortical circuits [Fig. 2(d); 8 connections among all 31 impaired connections], especially the connection between frontal areas and the thalamus, were also disrupted, in agreement with the VBA results showing a decreased FA in multiple WM regions in projection fibers. At the same time, eight homolateral subcortical connections mainly involving the right hippocampus, right thalamus and basal ganglia were disrupted in patients. Lastly, five intra-hemispheric connections involving widespread cortical regions were disrupted in patients, three in the right and two in the left hemisphere.

Table 3
Association of clinical variables with the mean FA values in significant clusters in patients.

	Region	r	p
PANSS-N	EC.R	−0.246	0.0032
PANSS-Total	EC.R	−0.231	0.0057
Duration	GCC + BCC	−0.294	0.0004
	PLIC.L	−0.251	0.0026
	GCC	−0.232	0.0057

Table 2
White matter areas with significantly lower FA values in patients than in healthy controls.

Region	Cluster size	MNI coord(Peak)	Peak T value	Mean FA	
				control	patient
Commissural fibers					
Genu of corpus callosum	284	[0 28–2]	6.83	0.563	0.547
Body and splenium of corpus callosum L	275	[−12–34 10]	7.07	0.506	0.487
Body and splenium of corpus callosum R	214	[12–34 10]	7.01	0.505	0.485
Genu and body of corpus callosum R	182	[16 40 6]	6.42	0.439	0.416
Projection fibers					
Cerebral peduncle L	73	[−14–14 -10]	6.60	0.561	0.544
Cerebral peduncle R	60	[16–14 -12]	6.16	0.545	0.523
Anterior limb of internal capsule R	45	[14 2 14]	6.03	0.485	0.468
Anterior limb of internal capsule L	41	[−20220]	6.76	0.491	0.469
Posterior limb of internal capsule L	40	[−18–6 2]	6.73	0.532	0.511
Association fibers					
Fornix	51	[0–4 12]	7.59	0.278	0.238
External capsule R	47	[32–14 10]	6.47	0.330	0.315
Tracts in the brainstem					
Superior cerebellar peduncle L	54	[−6–46 -26]	7.31	0.351	0.336
Superior cerebellar peduncle R	45	[6–46 -26]	7.49	0.358	0.342

FA, fractional anisotropy; MNI, Montreal Neurological Institute; L, left; R, right.

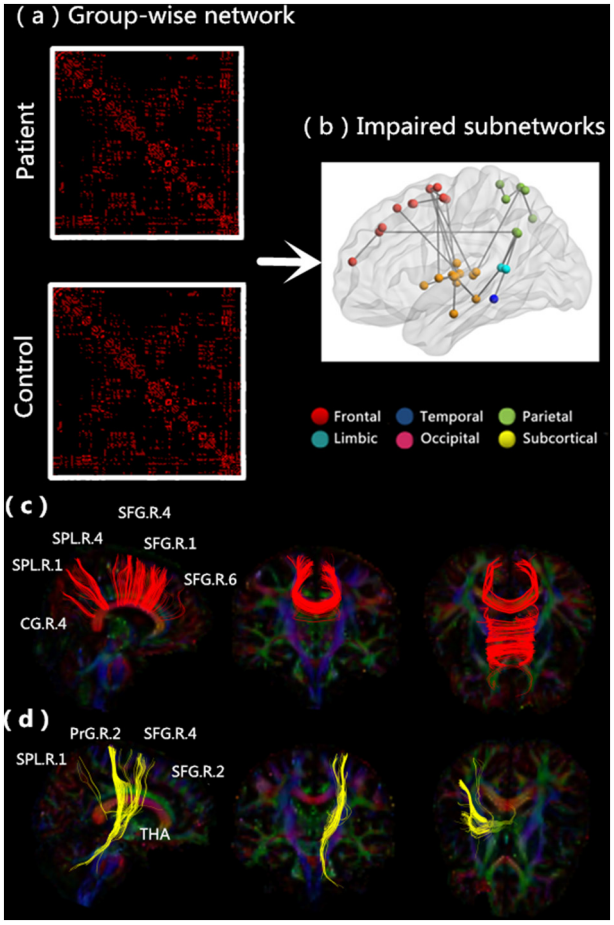

Fig. 2. Significantly changed inter-regional anatomical connections in patients with schizophrenia. (a) Group-wise network for all subjects obtained by carrying out a nonparametric one-tailed sign test. (b) Impaired subnetworks for patients with schizophrenia. Regions belonging to the frontal, temporal, parietal, limbic, occipital, and subcortical areas are color-coded in red, dark blue, green, blue, purple, and yellow, respectively. (c) Impaired interhemispheric connections. (d) Impaired thalamo-cortical feedback loops.(For interpretation of the references to color in this figure legend, the reader is referred to the web version of this article.)

3.3. Multivariate connectivity analysis

Small-world characteristics of the anatomical networks were tested for healthy subjects and patients with schizophrenia. We found that $\sigma > 1$ (Fig. 3) for both, indicating that small-world features exist in anatomical networks of both subject groups. For each subject, the values of K_p, S_p, E_{glob}, and E_{loc} values were calculated for the anatomical network. We found that all values were significantly lower in patients than in healthy subjects ($p = 8.95 \times 10^{-5}$, 1.10×10^{-3}, 3.00×10^{-5}, and 2.20×10^{-3} for K_p, S_p, E_{glob}, and E_{loc}, respectively).

3.4. Hub regions

Hub nodes include several central and highly connected areas, which participate in the global topology of the brain network. In this study, we used the nodal degree for determining these hub regions. Fig. 4 presents the detected hub regions in both healthy subjects and patients. The hub regions of patients were roughly identical to those of healthy individuals. These regions mainly included the basal ganglia (BG.L/R.2; BG.L/R.3; BG.L/R.6; BG.L.4), and thalamus (THA.L/R.8) (see Supplementary Table 1 for names and abbreviations). Two hubs were specific to patients, namely the left postcentral gyrus (PoG.L.4) and right superior frontal gyrus (SFG.R.1), while two regions were specific to healthy individuals, namely the left thalamus (THA.L.6) and right precuneus (PCun.R.3).

3.5. Network analysis robustness

Network analysis was repeated to determine the impaired connections using the same process *via* the AAL atlas. The inter-regional connections totaled 819 and 909 for patients and healthy subjects, respectively. The sparsity of SC for healthy subjects (0.2270) was 9.90% larger than that for patients (0.2045). The hub regions of patients were identical to those of control subjects, including the bilateral putamen, left thalamus, bilateral precuneus, and left calcarine. There were two subnetworks detected using the NBS method [$p = 0.05$, family-wise error rate corrected]: one subnetwork consisting of 15 connections ($p = 0$, corrected) and another consisting of 6 connections ($p = 0.023$, corrected). The details of all the 21 inter-regional connections are listed in Supplementary Table S5 and Supplementary Fig. 3. All of these connections were significantly lower in patients than in healthy individuals. Consistently with the BN-246 atlas, we found that half (12 among a total of 21 impaired connections) of the impaired interhemispheric connections involved connections between the left and right frontal and parietal regions: five concerned connections between the left and right frontal regions, five between parietal, and two between the right frontal and left parietal regions. Two subcortical-cortical connections were also identified. Regions that were mainly involved in the impaired connections included frontal (SMA; SFGmed; CG), parietal (SPG; PCUN; PCL; PoCG), and subcortical (THA) regions (see Supplementary Table 2 for names and abbreviations). Regarding the topological properties, we found that the AAL atlas' network parameters (K_p, S_p, E_{glob}, and E_{loc}) were similarly changed between patients and healthy individuals (Supplementary Table 6), as was the case for the BN-246 parameters.

4. Discussion

The present study provided evidence of WM disruptions in patients with schizophrenia, using a multilevel approach in a large sample size. VBA showed widespread decreases in FA values, with no regions showing increased FA values, consistently with a recent large sample meta-analysis on widespread FA-value reduction in schizophrenia (Kelly et al., 2017). Correlation analysis showed that some associaction fibers negatively correlated with negative scores on the PANSS. Fiber tracking also confirmed the observed FA-value reduction, as 31 connections were impaired in patients, especially the interhemispheric connections and thalamo-cortical feedback loops. Our topological property analysis suggests that the structural network of patients shows a weaker global integration and that their brain network hubs are less functional.

4.1. Interhemispheric connection

We found the most striking FA decreases in the corpus callosum. Meanwhile, fiber tracking also demonstrated impaired inter-hemispheric SC in frontal and parietal regions. Some studies have highlighted the corpus callosum and its postulated role, as part of the dysconnectivity hypothesis in schizophrenia. Our study offers additional evidence regarding the aberrant cerebral inter-hemispheric connectivity of callosal fibers, further strengthening the hypothesis that disrupted WM connectivity in the corpus callosum is important in the pathology of schizophrenia (Zalesky et al., 2011). Furthermore, structural and functional connectivity (FC) are related. A recent study (Roland et al., 2017) assessed FC before and after surgical resection of the corpus callosum in 22 patients and revealed a causal role for this structure in maintaining interhemispheric FC throughout the brain. Our study revealed that patients with schizophrenia show disruptions in the

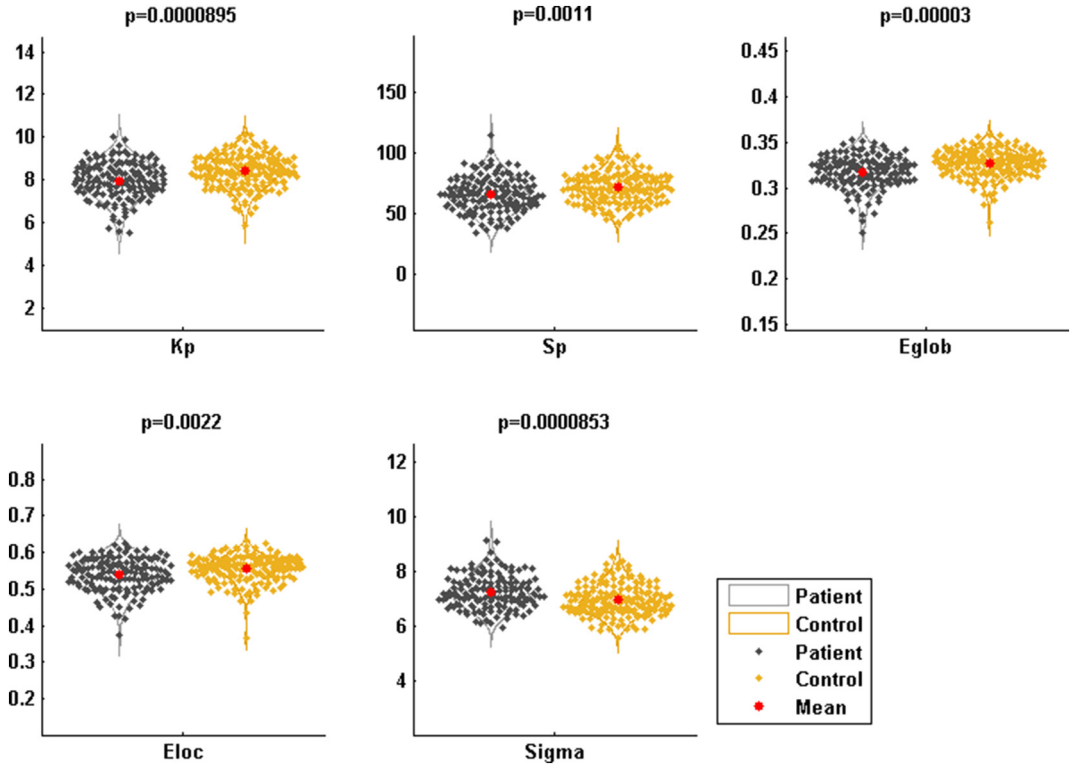

Fig. 3. Global parameters of the structural networks in patients and healthy individuals. The results were adjusted for motion score and age.

corpus callosum, thus providing structural evidence for the changes possibly underlying interhemispheric FC disruptions in schizophrenia (Guo et al., 2013; 2014; Chang et al., 2015). Previous behavioral research on inter-hemispheric interactions has demonstrated that functionally, it is more efficient if the two hemispheres interact than if one hemisphere performs all information processing (Belger and Banich, 1992). This is not surprising since inter-hemispheric interaction deficits may cause the sensory abnormalities, psychiatric symptoms, and cognitive deficits observed in patients with schizophrenia (Hoptman et al., 2012; Zhang et al., 2015a, 2015b).

Notably, using FA, we revealed a significant disruption in the splenium of the corpus callosum. The splenium encompasses interhemispheric connections between the occipital lobes and has been previously reported to exhibit abnormalities in patients with schizophrenia and to show the largest effect size regarding FA-value reductions (Patel et al., 2011; Sugranyes et al., 2012). In contrast, when we used fiber tracking, we did not detect any impairment in interhemispheric connections between the occipital lobes, which further highlights the importance of investigating WM disruptions at multiple levels.

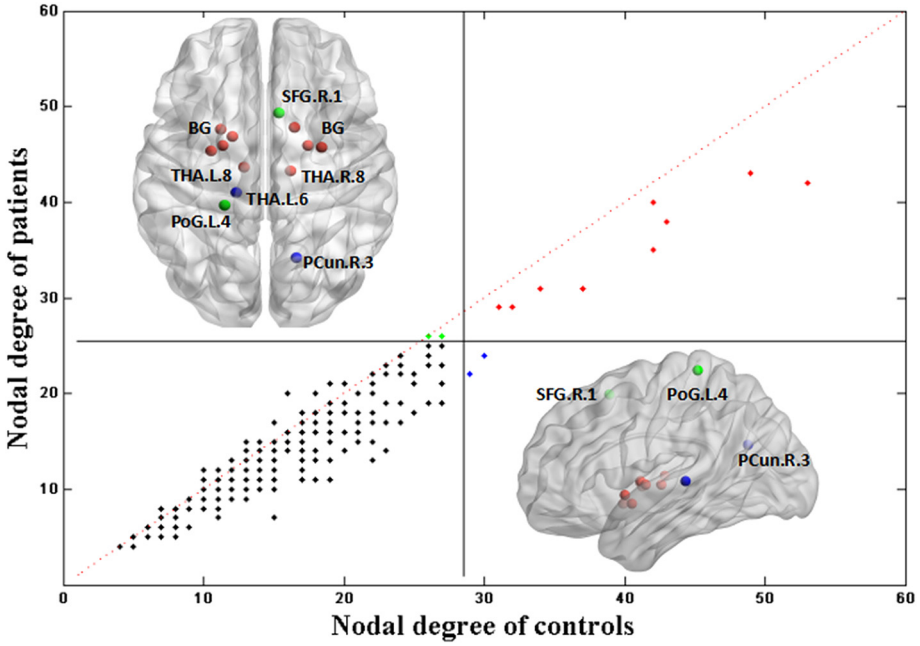

Fig. 4. Nodal degree of structural networks in patients with schizophrenia and healthy subjects. The horizontal and vertical lines correspond to the criterion values; 29 and 26 for healthy subjects and patients, respectively. Dots represent the 246 regions of the BN-246. Black dots, non-hub regions; red dots, hubs which appear in both subject groups; blue or green dots, hubs specific to healthy subjects or patients, respectively. See Supplementary Table 1 for names and abbreviations.(For interpretation of the references to color in this figure legend, the reader is referred to the web version of this article.)

4.2. Thalamo-cortical feedback loops

The thalamus is anatomically connected to limbic and cortical areas that are implicated in the development of schizophrenia symptoms (Adriano et al., 2010). Thus, it is an important area in the pathophysiology of schizophrenia as a whole (Rüsch et al., 2007). In this study, VBA revealed significant FA-value reductions in the ALIC and PLIC.L. Fiber tracking also showed five impaired connections between the thalamus and frontal regions, especially in the right hemisphere. Furthermore, the FA value in the ALIC negatively correlated with illness duration. These results are consistent with previous findings using different methods, including tract-based spatial statistics (Jeong et al., 2009) and probabilistic tractography approach (Kim et al., 2008). Similarly, many functional and structural MRI studies have also shown that the thalamus is an important area in schizophrenia. Cheng et al. (2015) conducted a regional analysis and voxel-based analysis to investigate altered brain-wide functional connectivity in large multisite samples. Their results show highly replicable aberrations in thalamo-cortical connectivity. Several structural MRI studies have also reported a significant volume reduction of the thalamus in patients with schizophrenia (see review Adriano et al., 2010). We also found that connections of the thalamus, as the hub of the structural network in our study, are also impaired. However, whether this is the basis for the functional or morphological disruptions found in patients with schizophrenia needs further verification. In contrast to the recent meta-analysis that showed the largest effect size in the anterior corona radiata (Kelly et al., 2017), we did not obtain significant results in this region after regression of head motion parameters and age. This may be because our sample size was not sufficient for this region to pass the multiple correction.

4.3. Network topological properties

In our study, we found small-world properties ($\sigma > 1$) in structural networks of the WM both in patients and healthy subjects, in agreement with the findings of several previous studies (Heuvel et al., 2010; Zhang et al., 2015a, 2015b). However, patients showed significantly decreased K_p and S_p values, indicating a reduction in axonal number or density, further suggesting reduction in the transformation of nerve pulses, which in turn leads to decreased information processing. The significantly lower E_{glob} and E_{loc} values found in patients with schizophrenia than in healthy subjects suggest that the local specialization and global integration capacity of processing parallel information possibly declines in WM structural networks in schizophrenia patients. In particular, previous studies have also shown reduced density and mean efficiency in patients with schizophrenia (Zalesky et al., 2011) and individuals with psychotic experiences (Drakesmith et al., 2015).

4.4. Hub regions

The hub regions detected in the control group using the nodal degree mainly included the basal ganglia, thalamus, superior frontal gyrus, and precuneus, highly consistent with previous studies (Heuvel et al., 2010), in which defined hubs were combined with four indexes, including nodal degree, closeness, betweenness centrality, and clustering coefficient. Ten of the detected hub areas were found in both groups, as shown in Fig. 4. However, all these regions showed a smaller nodal degree in patients than in healthy subjects. More importantly, some of these hub regions, especially the thalamus and precuneus, were also detected to have impaired connections, suggesting that they not only play a crucial role in the WM structural network, but are also vulnerable to damage in patients. Abnormalities in brain hubs are increasingly implicated in brain diseases and could potentially explain a wide range of schizophrenia symptoms (Crossley et al., 2014).

4.5. Limitations

Our study has certain limitations, which have to be taken into consideration and further addressed in the future. Firstly, we used diffusion deterministic tractography to draw the WM for the construction of the brain anatomical network, which, from a computational point of view, is simple and inexpensive and yields robust tractographic maps (Zalesky et al., 2011). However, based on previous research, deterministic tractography, as a tracking procedure, might show reduced ability to detect crossed fibers (Mori and van Zijl, 2002; Quan et al., 2013) or might not efficiently determine fiber orientation in areas with kissing, crossing, or twisting fiber tracts (Jbabdi and Johansenberg, 2011). The probabilistic tractography approach has the advantage of addressing the fiber crossing problem and thus could be a better choice for future research (Behrens et al., 2007). Secondly, the education level was different among participants; because of the disease, many patients suffered interrupted education. However, it is hard to find many patients and healthy individuals with the same education level. Therefore, we carried out a separate analysis to explore the correlation between education and the nodal degree or the FA maps; however, we did not find any significant correlation [$p = 0.1$ (FDR corrected)]. Thus, the difference in education between groups is possibly not an important confounding factor in the results. In future research, individuals of the same education level should be recruited. Thirdly, because our patients were all chronic schizophrenia patients, their history of medication was complex, so we carried out an analysis to explore the Spearman correlation between the dosage of chlorpromazine and the mean FA value of significant clusters; however, we did not find any significant correlation [$p > 0.2$ for all clusters]. Nevertheless, we cannot rule out the effect of drugs on WM injury. Lastly, although we obtained results from different templates, including hub regions, the results of graph theory and the identified impaired connections were consistent; however, there are still some inconsistencies, especially regarding the impaired thalamic connections. For example, based on the BN-246 atlas, we found many impaired thalamo-cortical connections and homolateral subcortical connections, while based on the AAL atlas, we only found two impaired connections involving the thalamus. Moreover, we could not detect any impairment in the connections within subcortical regions. This might be due to the fact that the thalamus is divided into 7 subregions in the BN atlas, thus network disruption might be easier to detect. Moreover, our results using the BN atlas also indicated some connections between the thalamus and frontal lobe with higher streamlines in patients with schizophrenia than in healthy controls. Nevertheless, these observations were not adequately significant to pass the multiple correction. In contrast, the AAL atlas does not separate the thalamus into subregions, and therefore, averages out the fine details over small spatial scales. As the AAL atlas seems to be used more widely, it is still difficult to determine which atlas is optimal. Thus, it is still unclear how to assess and control the influence of different atlases (Liu et al., 2015; Wang et al., 2012; Zalesky et al., 2010).

5. Conclusions

In conclusion, DTI is a useful tool to evaluate brain connectivity in schizophrenia. We found widespread WM connectivity disruptions in patients with schizophrenia, especially involving the inter-hemispheric connections and thalamo-cortical circuits, significantly associated with illness duration. In future studies, brain changes can be examined by combining multimodal data to further study the relationship between structural damages and functional and morphological disruptions, especially in relation to the inter-hemispheric connectivity and thalamic damage.

Funding

SXG is supported by the National Natural Science Foundation of

China (NSFC) grant (No.11671129), Natural Science Foundation of Hunan Province (2015JJ1010). CPL is supported in part by funding from Ministry of Science and Technology (104-2218-E-010-007-MY3, MOST 105-B-2633-400-001, and MOST 106-2321-B-010-011) and National Health Research Institutes, Taiwan (NHRI-EX106-10611EI).

Appendix A. Supplementary data

Supplementary data to this article can be found online at https://doi.org/10.1016/j.nicl.2018.08.027.

References

Adriano, F., Spoletini, I., Caltagirone, C., Spalletta, G., 2010. Updated meta-analyses reveal thalamus volume reduction in patients with first-episode and chronic schizophrenia[J]. Schizophr. Res. 123 (1), 1–14.
Andreasen, N.C., Arndt, S., Cizadlo, T., Flaum, M., O'Leary, D., Ehrhardt, J.C., et al., 1994. Thalamic abnormalities in schizophrenia visualized through magnetic resonance image averaging[J]. Science 266 (5183) (294–294).
Bassett, D.S., Bullmore, E., Verchinski, B.A., Mattay, V.S., Weinberger, D.R., Meyerlindenberg, A., 2008. Hierarchical organization of human cortical networks in health and schizophrenia[J]. J. Neurosci. Off. J. Soc. Neurosci. 28 (37), 9239–9248.
Bassett, D.S., Bullmore, E.T., Meyerlindenberg, A., Apud, J.A., Weinberger, D.R., Coppola, R., 2009. Cognitive fitness of cost-efficient brain functional networks. Proc. Natl. Acad. Sci. U. S. A. 106 (28), 11747–11752.
Bassett, D.S., Nelson, B.G., Mueller, B.A., Camchong, J., Lim, K.O., 2012. Altered resting state complexity in schizophrenia[J]. NeuroImage 59 (3), 2196–2207.
Baum, G.L., Roalf, D.R., Cook, P.A., et al., 2018. The impact of in-scanner head motion on structural connectivity derived from diffusion MRI[J]. NeuroImage 173.
Behrens, T.E., Berg, H.J., Jbabdi, S., Rushworth, M.F., Woolrich, M.W., 2007. Probabilistic diffusion tractography with multiple fibre orientations: what can we gain?[J]. NeuroImage 34 (1), 144–155.
Belger, A., Banich, M.T., 1992. Interhemispheric interaction affected by computational complexity[J]. Neuropsychologia 30 (10), 923–929.
Bora, E., Fornito, A., Radua, J., Walterfang, M., Seal, M., Wood, S.J., et al., 2011. Neuroanatomical abnormalities in schizophrenia: a multimodal voxelwise meta-analysis and meta-regression analysis[J]. Schizophr. Res. 127 (1–3), 46–57.
Bullmore, E.T., Bassett, D.S., 2011. Brain graphs: graphical models of the human brain connectome[J]. Annu. Rev. Clin. Psychol. 7 (7), 113.
Bullmore, E.T., Frangou, S., Murray, R.M., 1997. The dysplastic net hypothesis: an integration of developmental and dysconnectivity theories of schizophrenia. Schizophr. Res. 28 (2–3), 143–156.
Chang, X., Xi, Y.B., Cui, L.B., Wang, H.N., Sun, J.B., Zhu, Y.Q., et al., 2015. Distinct inter-hemispheric dysconnectivity in schizophrenia patients with and without auditory verbal hallucinations[J]. Sci. Rep. 5, 11218.
Cheng, W., Palaniyappan, L., Li, M., Kendrick, K.M., Zhang, J., Luo, Q., ... Ma, X., 2015. Voxel-based, brain-wide association study of aberrant functional connectivity in schizophrenia implicates thalamocortical circuitry[J]. npj Schizophrenia 1 (15016).
Crossley, N.A., Mechelli, A., Scott, J., Carletti, F., Fox, P.T., McGuire, P., Bullmore, E.T., 2014. The hubs of the human connectome are generally implicated in the anatomy of brain disorders[J]. Brain 137 (8), 2382–2395.
Cui, Z., Zhong, S., Xu, P., Gong, G., He, Y., 2013. PANDA: a pipeline toolbox for analyzing brain diffusion images[J]. Front. Hum. Neurosci. 7 (42), 1–16.
Deprez, S., Amant, F., Smeets, A., et al., 2012. Longitudinal assessment of chemotherapy-induced structural changes in cerebral white matter and its correlation with impaired cognitive functioning[J]. J. Clin. Oncol. Off. J. Am. Soc. Clin. Oncol. 30 (3), 274–281.
Domen, P.A., Michielse, S., Gronenschild, E., Habets, P., Roebroeck, A., Schruers, K., et al., 2013. Microstructural white matter alterations in psychotic disorder: a family-based diffusion tensor imaging study[J]. Schizophr. Res. 146 (1–3), 291–300.
Drakesmith, M., Caeyenberghs, K., Dutt, A., Zammit, S., Evans, C.J., Reichenberg, A., ... Jones, D.K., 2015. Schizophrenia-like topological changes in the structural connectome of individuals with subclinical psychotic experiences[J]. Hum. Brain Mapp. 36 (7), 2629–2643.
Fan, L., Li, H., Zhuo, J., Zhang, Y., Wang, J., Chen, L., et al., 2016. The human brainnetome atlas: a new brain atlas based on connectional architecture[J]. Cereb. Cortex 26 (8), 1–19.
Fitzsimmons, J., Kubicki, M., Shenton, M.E., 2013. Review of functional and anatomical brain connectivity findings in schizophrenia[J]. Curr. Opinion Psychiatr. 26 (2), 172–187.
Gong, G., He, Y., Concha, L., Lebel, C., Gross, D.W., Evans, A.C., et al., 2009. Mapping anatomical connectivity patterns of human cerebral cortex using in vivo diffusion tensor imaging tractography[J]. Cereb. Cortex 19 (3), 524–536.
Guo, W.B., Liu, F., Xue, Z.M., Gao, K., Wu, R.R., Ma, C.Q., et al., 2012a. Altered white matter integrity in young adults with first-episode, treatment-naive, and treatment-responsive depression. Neurosci. Lett. 522 (2), 139.
Guo, W., Liu, F., Liu, Z., Gao, K., Xiao, C., Chen, H., et al., 2012b. Right lateralized white matter abnormalities in first-episode, drug-naive paranoid schizophrenia. Neurosci. Lett. 531 (1), 5.
Guo, S., Kendrick, K.M., Zhang, J., Matthew, B., Yu, R., Liu, Z., et al., 2013. Brain-wide functional inter-hemispheric disconnection is a potential biomarker for schizophrenia and distinguishes it from depression[J]. Neuroimage Clin. 2 (1), 818–826.
Guo, W., Jiang, J., Xiao, C., Zhang, Z., Zhang, J., Yu, L., et al., 2014. Decreased resting-state interhemispheric functional connectivity in unaffected siblings of schizophrenia patients[J]. Schizophr. Res. 152 (1), 170–175.
Heuvel, M.P.V.D., Mandl, R.C., Stam, C.J., Kahn, R.S., Pol, H.E.H., 2010. Aberrant frontal and temporal complex network structure in schizophrenia: a graph theoretical analysis[J]. J. Neurosci. 30 (47), 15915–15926.
Hoptman, M.J., Zuo, X.N., D'Angelo, D., Mauro, C.J., Butler, P.D., Milham, M.P., et al., 2012. Decreased interhemispheric coordination in schizophrenia: a resting state fmri study[J]. Schizophr. Res. 141 (1), 1–7.
Jbabdi, S., Johansenberg, H., 2011. Tractography - where do we go from here?[J]. Brain Connectivity 1 (3), 169–183.
Jeong, B., Wible, C.G., Hashimoto, R.I., Kubicki, M., 2009. Functional and anatomical connectivity abnormalities in left inferior frontal gyrus in schizophrenia[J]. Hum. Brain Mapp. 30 (12), 4138–4151.
Karlsgodt, K.H., 2015. Diffusion imaging of white matter in schizophrenia: progress and future directions[J]. Biol. Psychiatr. Cogn. Neurosci. Neuroimag. 1 (3), 209–217.
Kelly, S., Jahanshad, N., Zalesky, A., et al., 2017. Widespread white matter microstructural differences in schizophrenia across 4322 individuals: results from the ENIGMA Schizophrenia DTI Working Group[J]. Mol. Psychiatry (5), 23.
Kim, D.J., Kim, J.J., Park, J.Y., Lee, S.Y., Kim, J., Kim, I.Y., et al., 2008. Quantification of thalamocortical tracts in schizophrenia on probabilistic maps[J]. Neuroreport 19 (4), 399–403.
Kong, X., Ouyang, X., Tao, H., Liu, H., Li, L., Zhao, J., et al., 2011. Complementary diffusion tensor imaging study of the corpus callosum in patients with first-episode and chronic schizophrenia. J. Psychiatry Neurosci. 36 (2), 120–125.
Kubicki, M., Mccarley, R., Westin, C.F., Park, H.J., Maier, S., Kikinis, R., et al., 2007. A review of diffusion tensor imaging studies in schizophrenia[J]. J. Psychiatr. Res. 41 (2), 15–30.
Liu, F., Guo, W., Fouche, J.P., Wang, Y., Wang, W., Ding, J., et al., 2015. Multivariate classification of social anxiety disorder using whole brain functional connectivity[J]. Brain Struct. Funct. 220 (1), 101–115.
Liu, J., Li, M., Pan, Y., Lan, W., Zheng, R., Wu, F.X., Wang, J., 2017. Complex brain network analysis and its applications to brain disorders: a survey. Complexity 2017.
Mori, S., van Zijl, P.C., 2002. Fiber tracking: principles and strategies - a technical review [J]. NMR Biomed. 15 (7–8), 468–480.
Mori, S., Crain, B.J., Chacko, V.P., van Zijl, P.C., 1999. Three-dimensional tracking of axonal projections in the brain by magnetic resonance imaging[J]. Ann. Neurol. 45 (2), 265–269.
O'Donoghue, S., Holleran, L., Cannon, D.M., McDonald, C., 2017. Anatomical dysconnectivity in bipolar disorder compared with schizophrenia: a selective review of structural network analyses using diffusion mri[J]. J. Affect. Disord. 209, 217–228.
Patel, S., Mahon, K., Wellington, R., Zhang, J., Chaplin, W., Szeszko, P.R., 2011. A meta-analysis of diffusion tensor imaging studies of the corpus callosum in schizophrenia [J]. Schizophr. Res. 129 (2), 149–155.
Peters, B.D., Blaas, J., De, H.L., 2010. Diffusion tensor imaging in the early phase of schizophrenia: what have we learned?[J]. J. Psychiatr. Res. 44 (15), 993–1004.
Quan, M., Lee, S.H., Kubicki, M., Kikinis, Z., Rathi, Y., Seidman, L.J., ... Levitt, J.J., 2013. White matter tract abnormalities between rostral middle frontal gyrus, inferior frontal gyrus and striatum in first-episode schizophrenia[J]. Schizophr. Res. 145, 1), 1–10.
Roalf, D.R., Ruparel, K., Verma, R., Elliott, M.A., Gur, R.E., Gur, R.C., 2013. White matter organization and neurocognitive performance variability in schizophrenia. Schizophr. Res. 143 (1), 172–178.
Roland, J.L., Snyder, A.Z., Hacker, C.D., Mitra, A., Shimony, J.S., Limbrick, D.D., et al., 2017. On the role of the corpus callosum in interhemispheric functional connectivity in humans[J]. Proc. Natl. Acad. Sci. 114 (50), 13278–13283.
Rüsch, N., Spoletini, I., Wilke, M., Bria, P., Di Paola, M., Di Iulio, F., ... Spalletta, G., 2007. Prefrontal–thalamic–cerebellar gray matter networks and executive functioning in schizophrenia[J]. Schizophr. Res. 93 (1), 79–89.
Samartzis, L., Dima, D., Fusar-Poli, P., Kyriakopoulos, M., 2014. White matter alterations in early stages of schizophrenia: a systematic review of diffusion tensor imaging studies[J]. J. Neuroimaging 24 (2), 101–110.
Stephan, K.E., Baldeweg, T., Friston, K.J., 2006. Synaptic plasticity and dysconnection in schizophrenia. Biol. Psychiatry 59 (10), 929–939.
Sugranyes, G., Kyriakopoulos, M., Dima, D., O'Muircheartaigh, J., Corrigall, R., Pendelbury, G., et al., 2012. Multimodal analyses identify linked functional and white matter abnormalities within the working memory network in schizophrenia[J]. Schizophr. Res. 138 (2–3), 136–142.
Tzourio-Mazoyer, N., Landeau, B., Papathanassiou, D., Crivello, F., Etard, O., Delcroix, N., et al., 2002. Automated anatomical labeling of activations in spm using a macroscopic anatomical parcellation of the mni mri single-subject brain[J]. NeuroImage 15 (1), 273–289.
Wakana, S., Jiang, H., Nagae-Poetscher, L.M., van Zijl, P.C., Mori, S., 2004. Fiber tract-based atlas of human white matter anatomy[J]. Radiology 230 (1), 77–87.
Wang, Q., Su, T.P., Zhou, Y., Chou, K.H., Chen, I.Y., Jiang, T., et al., 2012. Anatomical insights into disrupted small-world networks in schizophrenia[J]. NeuroImage 59 (2), 1085–1093.
Wang, J., Wang, X., Xia, M., Liao, X., Evans, A., He, Y., 2015. GRETNA: a graph theoretical network analysis toolbox for imaging connectomics. Front. Hum. Neurosci. 9, 386.
Wen, W., Zhu, W., He, Y., Kochan, N.A., Reppermund, S., Slavin, M.J., et al., 2011. Discrete neuroanatomical networks are associated with specific cognitive abilities in old age[J]. Journal of Neuroscience the Official Journal of the Society for. Neuroscience 31 (4), 1204–1212.
Winkler, A.M., Ridgway, G.R., Douaud, G., Nichols, T.E., Smith, S.M., 2016. Faster permutation inference in brain imaging[J]. NeuroImage 141, 502–516.
Yan, C.G., Wang, X.D., Zuo, X.N., Zang, Y.F., 2016. Dpabi: data processing & analysis for

(resting-state) brain imaging[J]. Neuroinformatics 14 (3), 339–351.
Yendiki, A., Panneck, P., Srinivasan, P., et al., 2011. Automated probabilistic reconstruction of white-matter pathways in health and disease using an atlas of the underlying anatomy[J]. Front. Neuroinformatics 5 (23), 23.
Yendiki, A., Koldewyn, K., Kakunoori, S., et al., 2014. Spurious group differences due to head motion in a diffusion MRI study.[J]. NeuroImage 88 (3), 79.
Zalesky, A., Fornito Abullmore, E.T., 2010. Network-based statistic: identifying differences in brain networks. NeuroImage 53 (4), 1197–1207.
Zalesky, A., Fornito, A., Harding, I.H., Cocchi, L., Yücel, M., Pantelis, C., et al., 2010. Whole-brain anatomical networks: does the choice of nodes matter?[J]. NeuroImage 50 (3), 970–983.
Zalesky, A., Fornito, A., Seal, M.L., Cocchi, L., Westin, C.F., Bullmore, E.T., et al., 2011. Disrupted axonal fiber connectivity in schizophrenia[J]. Biol. Psychiatry 69 (1), 80–89.
Zhang, J., Kendrick, K.M., Lu, G., Feng, J., 2015a. The fault lies on the other side: altered brain functional connectivity in psychiatric disorders is mainly caused by counterpart regions in the opposite hemisphere. Cereb. Cortex 25 (10), 3475.
Zhang, R., Wei, Q., Kang, Z., Zalesky, A., Li, M., Xu, Y., et al., 2015b. Disrupted brain anatomical connectivity in medication-naive patients with first-episode schizophrenia[J]. Brain Struct. Funct. 220 (2), 1145–1159.
Zhao, L., Tan, X., Wang, J., Han, K., Niu, M., Xu, J., et al., 2017. Brain white matter structural networks in patients with non-neuropsychiatric systemic lupus erythematosus. Brain Imag. Behav. 12 (1), 1–14.